

In two-dimensional co-ordinate systems, the radiation field of a line source $J(\vec{r}_0, t)$ posited at \vec{r}_0 is

$$\phi(\vec{r}, t) = \int_{-\infty}^{+\infty} G(\vec{r}, \vec{r}_0; t, t') \frac{\partial}{\partial t'} J(\vec{r}_0, t') dt' \quad (3)$$

where $G(\vec{r}, \vec{r}_0; t, t')$ is Green's function in the time domain

$$G(\vec{r}, \vec{r}_0; t, t') = \frac{C}{2\pi\sqrt{C^2(t-t')^2 - |\vec{r} - \vec{r}_0|^2}} H[C(t-t') - |\vec{r} - \vec{r}_0|] \quad (4)$$

and H is the Heaviside function, and C is the wave velocity in free space. The Green function has a long tail which means that we had to integrate the time of the whole history of the current [7] as shown in eqn. 4. However, in TDMEI, $J(\vec{r}_0, t)$ need not be the true current distribution, and can be chosen arbitrarily to obtain the measuring functions. Thus currents with special waveforms in time can be chosen to avoid the real integral, and to find the analytical solutions of eqn. 3. The measuring current applied in this Letter is

$$J(\vec{r}, t') = \begin{cases} \frac{2}{\tau} \left(\frac{\tau}{2} + t - t_0 \right) & t \in \left[t_0 - \frac{\tau}{2}, t_0 \right] \\ \frac{2}{\tau} \left(\frac{\tau}{2} - t + t_0 \right) & t \in \left[t_0, t_0 + \frac{\tau}{2} \right] \\ 0 & t \notin \left[t_0 - \frac{\tau}{2}, t_0 + \frac{\tau}{2} \right] \end{cases} \quad (5)$$

where τ and t_0 are selected constants. It is easy to obtain the explicit formula for the integral of time when eqn. 5 is substituted into eqn. 3. After the choice of measuring currents, a series of $\{\phi_m^m\}$ is obtained and substituted into eqn. 3. The MEI coefficients are then found through the least squares method.

From the above statement, it is clear that the difference between TDMEI and other ABCs is that the coefficients in TDMEI are determined numerically rather than analytically.

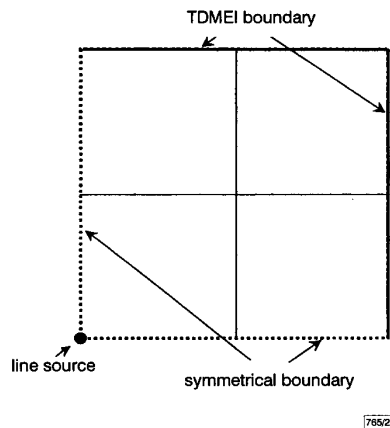


Fig. 2 Mesh for radiation of line source in Cartesian co-ordinates

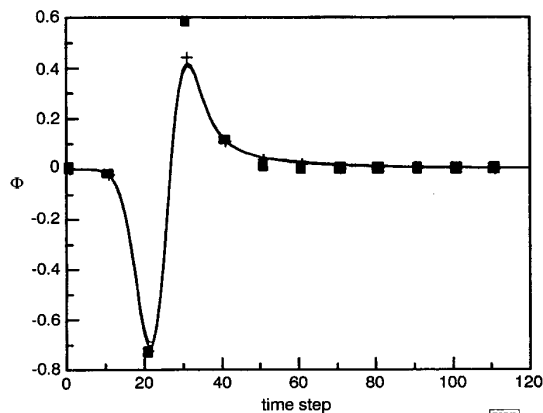


Fig. 3 Radiation of line source simulated by different methods

— TDMEI
 - - - exact
 + PML(8)
 ■ Mur2

Numerical tests: The radiation of a line source is simulated in 2D Cartesian co-ordinates. Owing to field symmetry, a quarter domain is computed, as shown in Fig. 2. To examine the validity of the TDMEI method, the truncated boundary is placed as close to the line source as possible. In our calculation, the truncated boundary is chosen as being only two space steps away from the line source. The measuring current is set as a line source at the same position as the real source and has the time waveform given in eqn. 5. Thus the measuring functions in eqn. 4 are obtained analytically, and then substituted into eqn. 3 to calculate the MEI coefficients at each node on the truncated boundary. The radiation of a real Gaussian pulse is then computed. Fig. 3 gives the waveforms at the middle node of the right truncated boundary of the real solution and the results of TDMEI, Mur's second order and eight layer PML ABCs. The TDMEI result is only slightly different from the real solution, better than the result of the eight layer PML and much better than the result of the Mur's second order ABC. It should be pointed out that the real number of layers for PML is 10, because eight absorbing layers had been used.

Conclusion: In this Letter, we have shown how to use the TDMEI method to derive the truncated boundary condition that allows us to terminate the computational domain so that it is as close to the line source as possible. Further research will extend the TDMEI method to the scattering problems of arbitrarily shaped conducting objects.

© IEE 1999

Electronics Letters Online No: 19990206

DOI: 10.1049/el:19990206

Yaowu Liu, Kang Lan, Cheng Liao and K.K. Mei (Department of Electrical Engineering, City University of Hong Kong, Kowloon, Hong Kong)

E-mail: eeliyu@cityu.edu.hk

4 January 1999

References

- 1 MEI, K.K., POUS, R., CHEN, Z.C., LIU, Y.W., and PROUTY, M.: 'Measured equation of invariance - a new concept in field computations'. Int. IEEE/AP-S Symp., Chicago, USA, 1992, pp. 2047-2050
- 2 MEI, K.K., POUS, R., CHEN, Z.C., LIU, Y.W., and PROUTY, M.: 'Measured equation of invariance - a new concept in field computations', *IEEE Trans.*, 1994, **AP-42**, (3), pp. 320-328
- 3 LIU, Y., YUNG, K.N., and MEI, K.K.: 'Interpolation, extrapolation and application of the measured equation of invariance to scattering by very large cylinders', *IEEE Trans.*, 1997, **AP-45**, (9), pp. 1325-1331
- 4 RIUS, J.M., POUS, R., and CARDAMA, A.: 'Integral formulation of the measured equation of invariance: A novel sparse matrix boundary element method', *IEEE Trans.*, 1996, **MAG-32**, (3), pp. 962-967
- 5 MEI, K.K.: 'Measured equation of invariance and its application in frequency and time domain'. EUROEM Dig., Bordeaux, France, June 1995, pp. 925-932
- 6 FAFLOVE, A.: 'Computational electrodynamics. The finite-difference time-domain method' (Artech House, Boston/London, 1995)
- 7 CHEW, W.C.: 'Waves and fields in inhomogeneous media' (Van Nostrand Reinhold, New York, 1990)

Class of multichannel image processing filters

L. Khriji and M. Gabbouj

A new class of multichannel image processing filters called vector median rational hybrid filters (VMRHF) for multispectral image processing is introduced and applied to the colour image filtering problem. These filters are based on rational functions. The rational function structure is attractive in filtering since it is a universal approximator and a good extrapolator. The VMRHF is a two stage filter, which exploits the features of the vector median filter and those of the vector rational operator. These filters exhibit desirable properties, such as edge and detail preservation and accurate chromaticity estimation.

Introduction: Multichannel image processing is studied in this Letter using a vector approach which is more appropriate than the

traditional approaches that have been addressed using componentwise operators. This is due to the inherent correlation that exists between the image channels. In vector approaches, each pixel value is considered as an m -dimensional vector (m is the number of image channels; in the case of colour images, $m = 3$). A number of vector processing filters usually involve the minimisation of an appropriate error criterion [1, 4]. One class of filters considers the distance in the vector space between the image vectors; a typical representative of this class is the 'vector median filter' (VMF) [1]. A second class of filters operates by considering the vectors' directions, and has the name 'vector directional filter' (VDF) [4]. A third class of filters operates using rational functions in their input/output relation, and hence is called the 'vector rational filter' (VRFs) [2].

In this Letter, a novel filter structure is introduced, the vector median-rational hybrid filter (VMRHF), which constitutes a natural extension of the nonlinear rational type hybrid filter called the median-rational hybrid filter (MRHF) recently introduced for 1D and 2D signal processing [3], based on rational functions.

The VMRHF is formed by three sub-filters (two vector median filters and one centre weighted vector median filter) and one vector rational operation. VMRHF's are very useful in colour (and generally multichannel) image processing, since they inherit the properties of their ancestors. They constitute very accurate estimators in long- and short-tailed noise distributions and, at the same time, they preserve the chromaticity of the image vectors. Moreover, they act in a small window and with few operations, resulting in simple and fast filter structures.

Vector median-rational hybrid filters: The output vector $\underline{y}(n)$ of the VMRHF is the result of a vector rational function taking into account three input sub-functions which form an input function set $\{\Phi_1, \Phi_2, \Phi_3\}$, where the 'central one' (Φ_2) is fixed as a centre weighted vector median sub-filter

$$\underline{y}(n) = \Phi_2(n) + \frac{\sum_{j=1}^3 \alpha_j \Phi_j(n)}{h + k \|\Phi_1(n) - \Phi_3(n)\|_2} \quad (1)$$

where $\|\cdot\|_2$ is an L_2 -vector norm and $\alpha = [\alpha_1, \alpha_2, \alpha_3]^T$ characterises the constant vector coefficient of the input sub-functions. In this approach, we have chosen very simple prototype filter coefficients which satisfy the condition $\sum_{i=1}^3 \alpha_i = 0$. In our study, $\alpha = [1, -2, 1]^T$. h and k are positive constants. The parameter k is used to control the amount of the nonlinear effect.

The sub-filters Φ_1 and Φ_3 are chosen for an acceptable compromise between noise reduction, edge and chromaticity preservation. It is easy to observe that this VMRHF differs from a linear lowpass filter mainly in scaling, which is introduced on the Φ_1 and Φ_3 terms. Indeed, such terms are divided by a factor proportional to the output of an edge-sensing term characterised by an L_2 -vector norm of the vector difference between the two vectors Φ_1 and Φ_3 . The weight of the vector median-operation output term is accordingly modified, to keep the gain constant. The behaviour of the proposed VMRHF structure for different positive values of k is as follows:

- (i) $k \approx 0$; the form of the filter is given as a linear lowpass combination of the three nonlinear sub-functions: $\underline{y}(n) = c_1 \Phi_1(n) + c_2 \Phi_2(n) + c_3 \Phi_3(n)$. Coefficients c_1 , c_2 , and c_3 are constants
- (ii) $k \rightarrow \infty$; the output of the filter is identical to the central sub-filter output and the vector rational function has no effect: $\underline{y}(n) = \Phi_2(n)$
- (iii) For intermediate values of k , the $\|\Phi_1(n) - \Phi_3(n)\|_2$ term perceives the presence of a detail and accordingly reduces the smoothing effect of the operator.

Therefore, the VMRHF operates as a linear lowpass filter between three nonlinear suboperators, the coefficients of which are modulated by the edge-sensitive component. The structure of the VMRHF is shown in Fig. 1, using two bidirectional vector median sub-filters.

Experimental results: The VMRHF has been evaluated, and its performance has been compared with the performance of the widely known multidimensional nonlinear filters VMF and DDF, using RGB colour images as test multidimensional data. The noise attenuation properties of the different filters are examined by utilising a part of a colour Lena image (256×256). The test image has been contaminated using various noise source models to assess

the performance of the filters under different scenarios: (i) impulsive noise (each image channel is corrupted independently using salt and pepper noise); (ii) Gaussian noise $N(0, \sigma^2)$; (iii) mixed Gaussian-impulsive noise (salt and pepper 2% in each component, and Gaussian $N(0, \sigma^2)$).

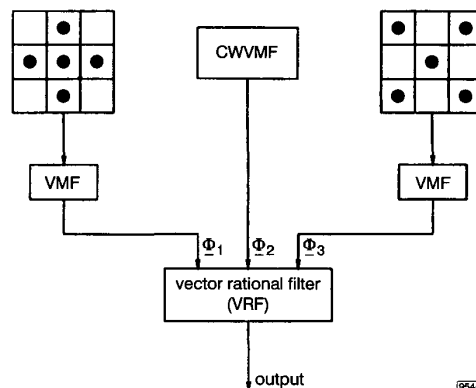


Fig. 1 Structure of VMRHF using two bidirectional vector median sub-filters

Table 1: Quantitative comparison

		Impulsive noise				
Filter	%	0.5	1	2	3	4
VMF	MAE	13.5	14.1	15.1	16.1	16.8
	MSE	173	186	204	228	247
	NCD	0.052	0.054	0.057	0.061	0.064
DDF	MAE	14.0	14.1	14.9	15.5	16.4
	MSE	196	203	219	235	261
	NCD	0.055	0.056	0.058	0.061	0.065
VMRHF	MAE	8.1	9.6	10.4	11.5	12.4
	MSE	74	99	124	184	234
	NCD	0.032	0.030	0.037	0.041	0.056
		Gaussian noise ($0, \sigma^2$)				
Filter	σ^2	50	100	200	300	400
VMF	MAE	17.9	20.7	24.8	28.1	31.1
	MSE	217	265	357	445	533
	NCD	0.079	0.095	0.120	0.140	0.157
DDF	MAE	20.1	23.9	29.4	33.5	38.0
	MSE	269	353	499	600	680
	NCD	0.091	0.113	0.150	0.169	0.187
VMRHF	MAE	15.1	18.6	22.6	25.7	28.5
	MSE	136	196	309	381	458
	NCD	0.070	0.085	0.107	0.126	0.143
		Mixed Gaussian-impulsive noise				
VMF	MAE	20.6	23.5	27.8	31.1	33.8
	MSE	280	336	446	544	636
	NCD	0.092	0.109	0.134	0.153	0.171
DDF	MAE	21.6	23.4	31.0	35.5	38.6
	MSE	314	402	550	705	810
	NCD	0.098	0.121	0.153	0.178	0.193
VMRHF	MAE	16.2	20.1	23.1	25.4	27.6
	MSE	182	250	319	389	447
	NCD	0.078	0.100	0.113	0.121	0.136

Three different objective measures have been used for quantitative comparison of the performance of the different filters: the mean absolute error (MAE), the mean square error (MSE), and the normalised colour difference (NCD). The latter measure is used to quantify the perceptual error between images in the perceptually uniform $L^*a^*b^*$ colour space. In the $L^*a^*b^*$ space, the L^* component defines the lightness, and the a^* and b^* components together define the chromaticity.

The results obtained are shown in Table 1 for the three noise models: impulsive, Gaussian, and Gaussian mixed with impulsive, respectively. As can be verified from these results, the performance of the new VMRHF is superior to the performance of the VMF and DDF. Moreover, consistent results have been obtained when using a variety of other color images and the same evaluation procedure. Considering the number of computations required for the

implementation of the VMRHF, it should be noted that it is comparable of those for the VMF. The vector rational operation does not introduce significant additional computational cost (a small look-up table for the denominator, one multiplication, three additions and one division per output sample).

Conclusions: A new class of nonlinear vector rational type hybrid filters for multidimensional image processing has been introduced. The vector median-rational hybrid filter is a vector rational operation of three sub-filters in which the central one is a centre weighted vector median filter. These filters exploit, in an effective way the features and the robustness of both vector median filters and vector rational filters. Simulation results and subjective evaluation of the filtered images indicate that the VMRHF's outperform all other filters under consideration. Moreover, as can be seen from the NCD results, the VMRHF's preserve the chromaticity component.

© IEE 1999
Electronics Letters Online No: 19990250
 DOI: 10.1049/el:19990250

23 November 1998

L. Khriji and M. Gabbouj (*Signal Processing Laboratory, Tampere University of Technology, PO Box 553 FIN-33 101 Tampere, Finland*)

E-mail: lazhar@cs.tut.fi

References

- 1 ASTOLA, J., HAAVISTO, P., and NEUVO, Y.: 'Vector median filter', *Proc. IEEE*, 1990, **78**, pp. 678-689
- 2 KHRJI, L., CHEIKH, F.A., and GABBOUJ, M.: 'High resolution digital resampling using vector rational filters', accepted for *J. Opt. Eng.* (Special Issue on Sampled Imaging Systems), May 1999
- 3 KHRJI, L., and GABBOUJ, M.: 'Median-rational hybrid filters'. Int. Conf. on Image Processing ICIP'98, Chicago, Illinois, USA, 4-7 October 1998
- 4 TRAHANIAS, P.E., KARAKOS, D., and VENETSANOPOULOS, A.N.: 'Directional processing of color images: Theory and experimental results', *IEEE Trans. Image Process.*, 1996, **5**, (6), pp. 868-880

Fast wavelet-based corner detection technique

A. Quddus and M.M. Fahmy

An improved, wavelet-based technique for corner detection in 2D planar curves is presented. This boundary based technique is simple to implement and computationally efficient and exploits the wavelet transform modulus maxima to detect corners. The proposed algorithm is robust with respect to object geometry. Results for noisy conditions are also reported.

Introduction: Corners in digital images give important clues for shape representation and analysis [1]. A multiresolution representation provides a simple hierarchical framework for interpreting the input image information [2]. Techniques based on scale space filtering are not computationally efficient because they require filtering with Gaussian functions over continuous scales. Wavelet theory provides a unified framework for a number of techniques which have been developed independently for various signal processing applications. In [3] a derivative of the Gaussian function is used as a wavelet. However, the derivative of the Gaussian function is not orthogonal and a fast computational algorithm for dyadic decomposition does not exist. In [4] a fast wavelet (given by Mallat [5]) is used to detect corners in 2D planar curves. However, this technique requires splitting the orientation profile and computing the derivative of the ratios of the wavelet transform modulus maxima (WTMM). In this Letter we propose a wavelet based algorithm which does not require these complex steps.

Choice of wavelet: Let the input signal be rewritten as $D = (S_j f(n))_{n \in \mathbb{Z}}$. We denote

$$W_{2^j}^d f = (W_{2^j} f(n + \omega))_{n \in \mathbb{Z}} \quad (1)$$

and

$$S_{2^j}^d f = (S_{2^j} f(n + \omega))_{n \in \mathbb{Z}} \quad (2)$$

where ω is the sampling shift that depends only on the wavelet $\psi(x)$. For any coarse scale 2^j , the sequence of discrete signals

$$\left\{ S_{2^j}^d, (W_{2^j}^d f)_{1 \leq j \leq J} \right\} \quad (3)$$

is called the discrete dyadic wavelet transform of $D = (S_j f(n))_{n \in \mathbb{Z}}$.

From the discrete wavelet transform, at each scale 2^j , modulus maxima are detected by finding the points where $|W_{2^j} f(n + \omega)|$ is larger than for its two closest neighbours and strictly larger than for at least one of them. The abscissa $n + \omega$ and the value $W_{2^j} f(n + \omega)$ at the corresponding locations are recorded.

A remarkable property of the wavelet transform is its ability to characterise the local regularity of functions [6]. In mathematics, local regularity is often measured with Lipschitz exponents. In [5], Mallat and Zhong proved that Lipschitz regularity can be accurately measured from WTMM if the wavelet used is a derivative of the Gaussian function. They also proposed a quadratic spline wavelet which is computationally efficient and quite similar to the derivative of the Gaussian. These properties make this wavelet a good choice for corner detection applications.

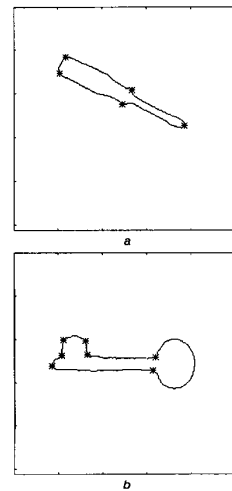


Fig. 1 Corner detection results

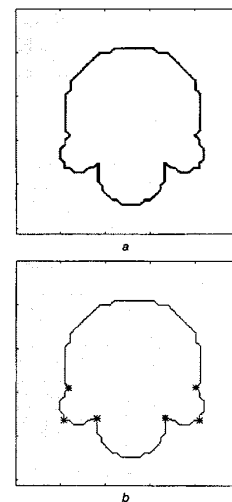


Fig. 2 Corner detection results

(a) Test image
 (b) Detected corners

Corner detection scheme: The preprocessing steps are the same as those in [4]. This preprocessing gives the orientation profile (orientation of the tangent along the boundary contour) from the input image. Lee *et al.* [7] presented an analysis of the behaviour of wavelet transform modulus maxima with different corner models